# AN INNOVATIVE ELASTO-PLASTIC ENERGY DISSIPATOR FOR THE STRUCTURAL AND NON-STRUCTURAL BUILDING PROTECTION

**Xavier CAHÍS[1], Lluís TORRES[2] And Luis BOZZO[3]**

## SUMMARY

This paper presents a new steel shear link dissipador fabricated without welding in areas where yielding takes place, and making possible to design very small web thickness devices. The yielding part of the device is milled from one piece of rectangular shaped steel bars.

Four shear link specimens have been tested. This particular set of dissipators were developed for the protection of nonstructural walls. The characterization tests consisted in cyclic loading under displacement control at quasi-static mode. The specimens start dissipating energy from 0.5 mm of displacement and from loads of 14.45 KN. All dissipators develop large deformations without web buckling, with a total accumulate displacement over 420 mm and an average shear strain from 0.11 to 0.16 rad before first damage in the web. Dissipated energy goes from 10 to 21 KJ, and specimens dissipate an additional amount of energy after first web damage because their thick and narrow flanges and stiffeners. Consequently, this new device has a two mode response which results in a very robust and safe dissipator.

Proposed numerical models and simple mathematical expressions offer good results as compared to the experimentally obtained values. Values obtained with the equation presented by Kasai and Popov [1986] to determine buckling in shear stiffened links have been compared with numerically determined ones, with less than 6% of difference between them.

Experimental analysis in a SDOF system has been performed with the shear link dissipator, in a 4x4 m shaking table (ISMES laboratories - Italy). Numerical most significant values obtained with a simple numerical model differ less than 10% from experimental data.

## INTRODUCTION

From experimental and numerical studies, masonry partitions add significantly to the stiffness of a frame and alter its damping characteristics. Neglecting them in the analysis model is not a satisfactory design practice. However, presently it is very difficult to take advantage of their stiffness and strength since the masonry infill walls usually cannot resist large frame deformations resulting that buffeting from the frame destroys the partitions.

Limiting the drift is the most wide spread solution to protect building equipment and nonstructural components. In general, codes specify drift limits such as a percentage of a story height. A proper earthquake resistant design of a building should guarantee that, at each story, the drift limit is not exceeded, protecting the infill walls from excessive deformations and brittle failures. Another proposed solution for masonry wall protection is the uncoupling of the resistant structure from the infill walls providing a gap filled with foam rubber or other flexible inexpensive material. This avoids the introduction of uncertainties in the numeric model used for the design of the frame. The technique, however, does not take advantage of the stiffness and strength of the walls. Besides, if the bare frame is flexible and the ground motion is severe, buffeting may not be avoided destroying

[1] *Department of Industrial Engineering, University of Girona, Spain Email: cahis@watt.udg.es*
[2] *Department of Industrial Engineering, University of Girona, Spain*
[3] *Department of Industrial Engineering, University of Girona, Spain*

the partitions. A third technique couples the infill walls and the surrounding frames reinforcing the walls and their connections. There are experimental and numeric studies that indicate that the coupling is beneficial for the resisting structure [Brokken and Bertero, 1981]. This technique, however, requires additional workmanship for the connection of the walls and the frames, and it may not be economical for countries where labor is expensive. A different alternative proposed by Yanev and Mc Niven [1985] is to couple the infill walls and the resisting elements by using specially designed metal springs. This alternative incorporates a gap between the wall and the surrounding frame (as in the second alternative) and it connects the walls to the frames (as in the third one) using metal springs separated at certain intervals. The springs have a limited strength, smaller than the infill wall capacity. Numerical and experimental studies indicate that these connections can efficiently protect the walls limiting the size of the force transmitted to them by stiffening the frame for a certain effective amount. This paper proposes to replace the metal springs proposed by Yanev and Mc Niven by stiff energy dissipation devices to protect the walls and, at the same time, to take advantage of the well-established properties of passive control. The coupling is advantageous not only since the frame would increase its stiffness and strength but because the installation of the dissipators is simplified. An additional benefit of the proposed concept is its flexibility as, presently, most of the energy dissipation devices are located at the diagonal bracing systems which implies geometric restrictions such as, for example, width to height span ratios.

Most existing devices require large structural drifts in order to effectively reduce seismic response [Bozzo et al., 1996]. Consequently, the initial part of this research consisted in developing a new stiff energy dissipator device suitable for nonstructural protection. The new shear link (SL) devices developed have high stiffness in its elastic mode, but a limited strength and small yielding deformation and they can be used as a connector between masonry walls and the main frame. A recent research have proposed an aluminum SL, which has been manufactured with thin welded plates obtaining also small yielding loads [Rai and Wallace, 1998]. The proposed dissipator, however, is fabricated from one milled piece, making possible to design a variety of shapes with alternative energy dissipation modes. The manufacturing process avoids brittle behavior on welded parts and the local changes of mechanical properties caused by temperature effects. In large scale manufacturing the procedure saves expensive quality control needed in welded parts, and it can take advantage of advanced manufacturing techniques as CAD/CAM, which involve design flexibility, specimens repeatability and low costs as compared with procedures with much more workmanship involved.

Hysteretic shear yielding behavior of steel has been widely studied in the last twenty years. Shear web buckling under seismic excitations may be a source of device instabilities, but there are available various design guidelines such as those proposed by Kasai and Popov [1986] for standard I shaped stiffened steel shear links as well as those geometric link parameters as the size and stiffener distribution included in the Uniform Building Code [ICBO, 1997]. In particular, shear links in the eccentrically braced frames have offered stable hysteretic loops when the web have been properly stiffened [Roeder and Popov, 1978].

## EXPERIMENTAL BEHAVIOR ON TICK FLANGED SHEAR LINK DISSIPATOR

### Tests specimens

The specimens have an I shaped cross area with thick and narrow flanges. The main dissipating part has been milled from a one steel piece of structural rectangular shaped profile. Figure 1 and table 1 show, respectively, the geometry and the values of the parameters which differ in the four specimens, where a is the stiffener thickness, e is the web thickness and r is the radius between flanges/stiffeners and the web. The mechanical properties of the specimens are given in table 2, where $\sigma_y$ is the yield stress, $\sigma_u$ is the ultimate stress, E is the Young's modulus and $\varepsilon_u$ is the ultimate strain.

### Loading set up and instrumentation

Four specimens have been tested at ISMES (Bérgamo, Italy) using a 25 kN horizontal loading machine (figure 2). The characterization machine has an horizontal travelling head loaded by two servo-controlled and load cell equipped jacks, and a vertically travelling head moved by a jack equipped with a pressure transducer. Samples have been firmly subjected to the heads of the testing machine by 8 pre-stressed M22 8.8 bolds, and to detect any slide in both plate assemblies two displacement transducers between plates and heads have been provided. Loading tests has been programmed to keep coupling plates of the device parallel and equidistant. The cycling loading has been done in quasi-static conditions (0.3 mm/s) with an increasing amplitude of 1 mm per cycle. In the C device test procedure, first cycle amplitude has been higher (2 mm) than in the other tests (1 mm) and also a lower velocity has been used (0.05 mm/s) in order to determine more precisely the first yielding deformation (figure 2b).

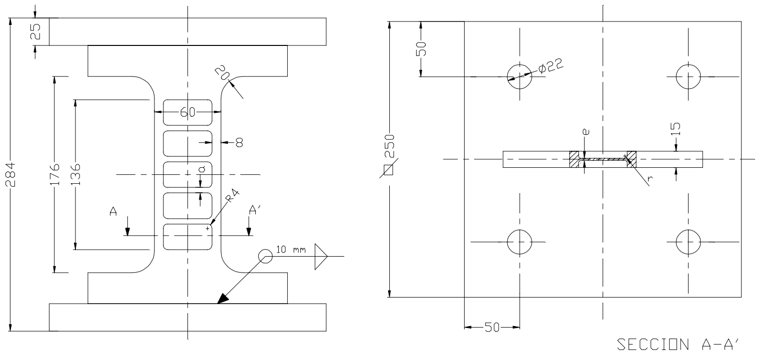


**Figure 1. Shear link dissipator manufacturing drawings used for the tests specimens**

**Table 1. Geometric variations between models**

| Model | a (mm) | e (mm) | r (mm) |
|---|---|---|---|
| A-device | 5 | 2 | 0 |
| B-device | 5 | 2 | 2 |
| C-device | 5 | 1.5 | 2 |
| D-device | 2.5 | 2 | 2 |

**Table 2. Steel properties**

| STEEL | $\sigma_y$ (MPa) | $\sigma_u$ (MPa) | E (MPa) | $\varepsilon_u$ (mm/mm) |
|---|---|---|---|---|
| Fe360B | 339.1 | 512.0 | $2.06\ 10^5$ | 0.201 |

(a)

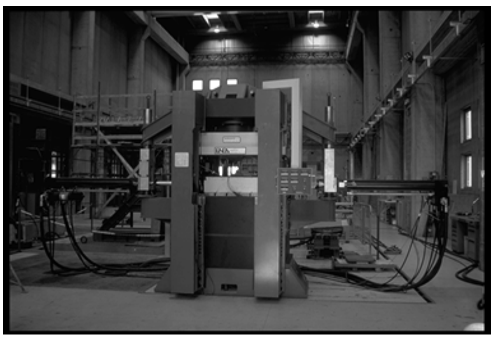

(b)

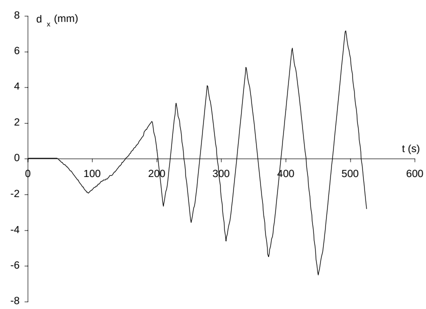


**Figure 2. (a) Characterization machine. (b) Displacement controlled vs. time used for testing C-device.**

## 2.3 Experimental results

The hysteretic curves for the four devices are very similar and all present a stable behavior with no bucking involved. As an example, figure 3(a) presents the load versus displacement relationship obtained from the C-specimen test. The figure 3(b) represents the time evolution of the total dissipated energy of this device. First damage has been identified by lose of dissipation capability (indicated as (2) in the figure), and it has happened in the four devices after the maximum horizontal load has been achieved (indicated as (1) in the figure).

After web damage has appeared, all devises dissipate an additional amount of energy. This is because the flanges and stiffeners are not damaged and they are thick and narrow dimensioned. In the full restrained vertical displacement model, this sub-structure maintains dissipating energy by bending as well as by axial loads originated, the later one, by second order large displacement effects. This behavior characteristic can be observed in figure 4(a) for specimen A, before and after the degradation of the web.

On table 3 main results are summarized, where $F_{x,y}$ is the first horizontal yielding load, $d_{x,y}$ is the first yielding displacement, $F_m$ is the maximum horizontal load, $F_{m,0}$ is the maximum horizontal load at null displacement, E is the total dissipated energy before web damage, and $d_T$ is the total absolute cumulative horizontal displacement before web damage. In the same table, some non-dimensional parameters have been defined: $\phi_{m,0} = F_{m,0}/F_{y,t}$ , $\varphi = E/(F_{m,0} \cdot d_T)$, and $\gamma_T = d_T/H$, where H is the distance between two web borders.

(a) (b)

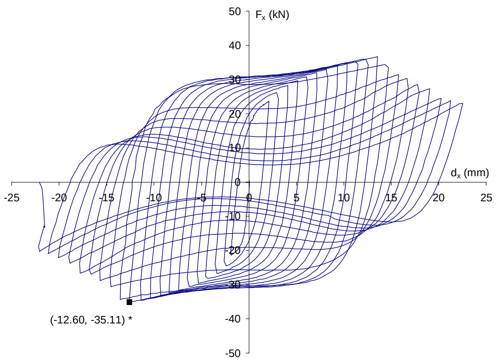


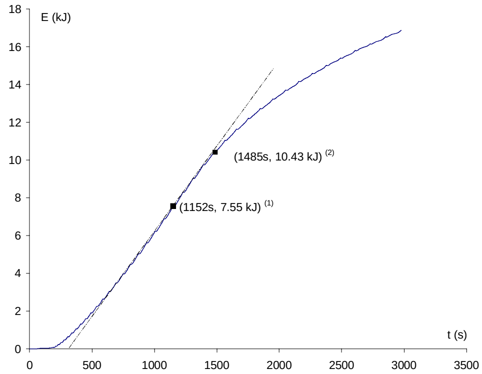


**Figure 3. (a) C-device load versus displacement hysteretic relationship (b) Evolution of the total dissipated energy of the 'C' specimen**

(a) (b)

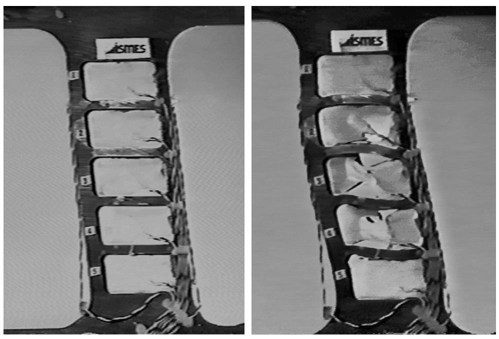

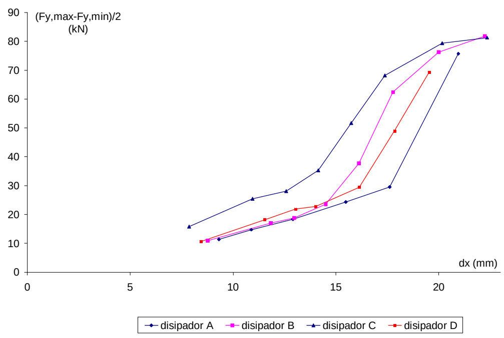


**Figure 4(a) A-device before an after web damage occurs. (b) Maximum cycle vertical force (semi-sum) versus displacement in the four devices**

**Table 3 Experimental values for the considered main parameters**

| | $F_{x,y}$ (kN) | $d_{x,y}$ (mm) | $F_m$ (kN) | $F_{m,0}$ (kN) | E (kJ) | $d_T$ (m) | $\phi_{m,0}$ | $\varphi$ | $\gamma_T$ |
|---|---|---|---|---|---|---|---|---|---|
| A | - | - | 43.46 | 37.95 | 21.28 | 0.731 | 1.965 | 0.768 | 5.375 |
| B | - | - | 42.35 | 37.94 | 15.16 | 0.517 | 1.964 | 0.767 | 3.801 |
| C | 14.45 | 0.538 | 35.88 | 30.83 | 10.43 | 0.426 | 2.01 | 0.791 | 3.132 |
| D | - | - | 40.28 | 34.98 | 15.62 | 0.563 | 1.811 | 0.793 | 4.140 |

The parameter $\phi_{m,0}$ does not take into account non-geometric influence, and it presents an average value of 1.9375, with a maximum difference of 0.12 between this value and the obtained in the 'D' device. This one has the thinnest dimensioned stiffeners of all the specimens. It may be interesting a performance of new tests on standard I shaped links to see the effect of flange/stiffeners size on this parameter. The parameter φ has a meaning of efficiency of the developed dissipator as compared with perfect elasto-plastic dissipator. The average value for the tested devices is 0.78 with a maximum difference respect the average of 0.013. $\gamma_T$ represents de average absolute cumulative angular strain. The 'A' device presents the highest value of the fourth, indicating that the transition radius does not improve hysteretic behavior of the dissipator. An acceptable reason would be that it causes the reduction of web area with uniform thickness, where dissipation takes place. This observation seems clear when the ratio r/b is large, but and extensive test program have to be done to confirm it.

It is clear than when large displacements are involved and vertical displacement is restrained, axial forces ought to appear. Not as obvious but experimentally found is that when first damage occurs to the web, specimens vertical response evolution inflects and higher vertical reactions are produced. Figure 4(b) illustrates the evolution of semi-sum for the two maximum vertical reactions obtained for each cycle at its maximum displacement, and it shows clearly the inflection.

## NUMERICAL BEHAVIOR ON TICK FLANGED SHEAR LINK DISSIPATOR

### Prediction mathematical models

#### *Displacement and load when device first yielding*

Von Mises criteria has been used for the yielding prediction, and elastic small-deflection beam theory has been applied to calculate normal and shear stresses:

$$\sigma=\frac{M\ x}{I} \tag{1}$$

$$\tau=\frac{V\,S}{I\ t_w} \tag{2}$$

For displacement first yielding prediction, bending and shear deformation is included:

$$d_x=\left[\frac{H^3}{12EI_y}+\frac{H'}{A_wG}\right]V \tag{3}$$

Where σ is the cross area normal stress, τ is the cross area shear stress, dx is the horizontal displacement between both device coupling plates, M is the bending moment, V is the transverse shear force, x is the distance from neutral axis of bending, $t_w$ is the web thickness, I is inertial moment from neutral axis of bending, S is the first half area moment from neutral axis of bending, E is the Young's modulus, G is the shear elastic modulus, $A_w$ is the web cross area, H is the length of I shaped part of the dissipator, and H' is the effective length (H' = H – n e, where n is the number of stiffeners and e its thickness).

#### *First buckling prediction models and stiffeners considerations*

Kasai and Popov [1986] presented the following expression for buckling prediction in I shaped and stiffened shear links

$$\gamma_{m,b}=8.7K_S(\alpha)\left(\frac{1}{\beta}\right)^2 \tag{4}$$

where the parameter $\gamma_m$ is graphically defined in figure 5, and $\gamma_{m,b}$ is its corresponding buckling value. Clamped borders condition was assumed for the web, with $Ks = 5.6 + 8.98/\alpha^2$ when $0\leq\alpha\leq1$ (Bleich, 1952). Non-dimensional parameters are defined as $\alpha = a/b$ and $\beta = b/t_w$, where 'a' and 'b' are, respectively, the stiffener spacing and the clear distance between flanges.

#### *FEM based numerical models*

The vertical reactions obtained for the non-degraded model have been compared to the ones from a simple full web degraded model (figure 7a represents this model, and figure 7b the obtained graphical comparison). A lower vertical force evolution has been obtained in the former, so when damage occurs to the web, the vertical load response has to increase, as it has been noticed in the experimental results.

For buckling FEM prediction, a new dimensioned model has developed. It is milled from 90 x 10 mm rectangular bar. The provided thickness for the web, the flanges and the stiffeners are respectively 1.5 mm, 8 mm and 5 mm. The uniform spacing of the two introduced stiffeners is 40 mm. A difference of 5.7 % has been found between displacement obtained from equation 4 and the numerical results.

(a)

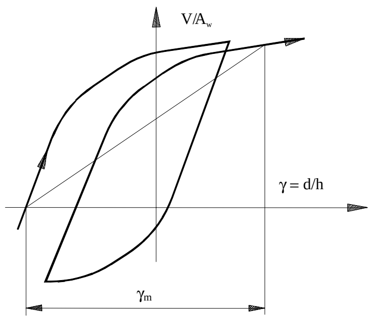


(b)

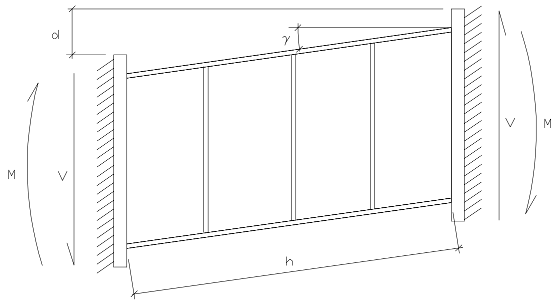


**Figure 5 (a) Average shear strain - link deformation angle relationship. (b) Deformed shear link element.**

(a)

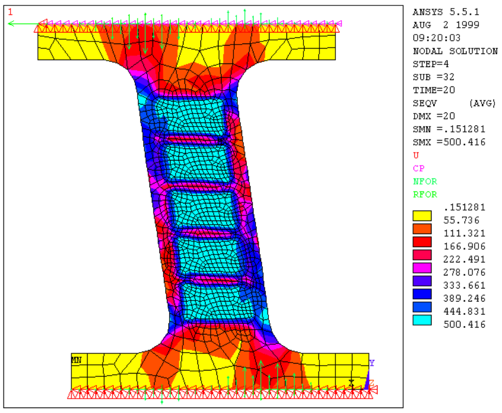


(b)

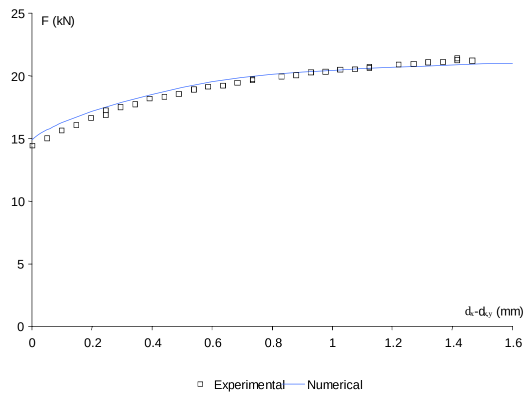


**Figure 6(a) Finite element model for thick SLD with von Mises stress distribution at $d_x$=20mm. (b)Numerical - experimental comparison for $F_x$ - $d_{x,plastic}$ for C device**

**Table 4 Load and displacement at yielding from numerical and experimental results in C device.**

| | experimental | simple models | FEM |
|---|---|---|---|
| $d_{x,y}$ (mm) | 0.547 | 0.41 | 0.39 |
| $F_{x,y}$ (kN) | 14.45 | 14.69 | 14.61 |

(a) (b)

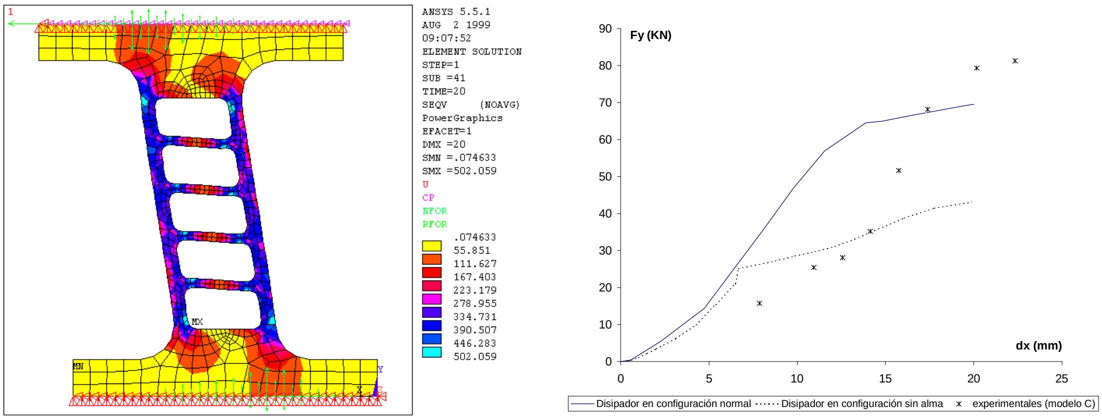


**Figure 7(a) Finite element model SLD without web, at 20 mm displacement, with von Mises stress distribution. (b) Numerical - experimental comparison for $F_y$ - $d_x$ for C device**

## BEHAVIOR OF A SDOF SYSTEM: EXPERIMENTAL AND NUMERICAL ANALYSES

A series of dynamic unidirectional tests have been performed for a single - story one bay full scaled frame. The frame has been connected to two reinforced concrete walls with the 'A' specimen (figure 8a). The model main characteristics are a total weigh of 8.4 tones and a period of 0,49 seconds for the bare frame. Before both shear links have been connected, the period turns 0.1 seconds and global damping 5%. Tests have been performed at 1.8 scaled Loma Prieta Earthquake. Figure 8(b) represents the obtained displacement of the top frame. The analysis of the data gives a total dissipated energy of 1.86 kJ (1/11 of the 'A' device capability obtained from its characterization test) with a maximum displacement of 6.54 mm on top frame. During the tests no torsional behavior has been involved. Stable dissipation mode has been observed in the devices. After testing, not damage has been appreciated in both the device and the main frame.

A numerical approach has been done, with the non-linearityes concentrated in the dissipator (as it happened experimentally). A very simple mathematical model, $F = F_y\ (d/d_y)^n$, has been used to simulate the hysteretic behavior of the shear link, where F is the load at displacement at displacement 'd', $F_y$ is the first yielding load, $d_y$ is the displacement at first yielding and n is and exponent to define the non linear behavior of the link. To obtain good correlation with experimental results, the concrete reinforced wall stiffness has been considered [Cahis et. Al. 1998]. A comparison between numerical and experimental results can be seen in table 5. Difference on maximum displacement on top frame was under 2%, while difference on total dissipated energy was 10%.

(a) (b)

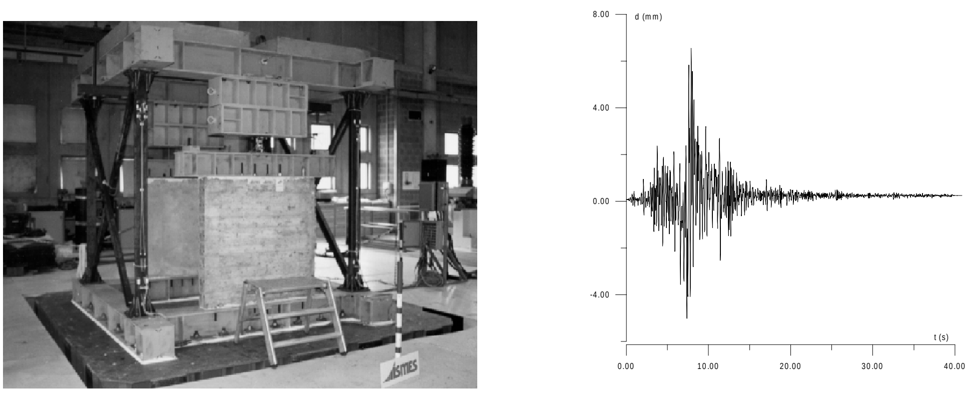


**Figure 9(a) SDOF model used for dynamic analysis (ISMES Laboratories, Italy). (b) Top frame displacement under 1.8 scaled Loma Prieta Earthquake**

**Table 5. Comparison between experimental and numerical results of SDOF analyses**

| | $d_{max}$ (mm) | $E_D$ (kJ) | $F_{max}$ (kN) |
|---|---|---|---|
| Experimental results | 6.54 | 1.86 | 43.06 |
| Numerical results | 6.43 | 2.05 | -39.82 |

## CONCLUSIONS

The main characteristics for the one piece milled shear link dissipator are: a) it presents high stiffness in the elastic range, b) its manufacturing process makes possible thin and small cross web areas with small yielding loads when proper material is used and c) due to these characteristics, very small displacements are required for first yielding. It seems appropriate for protecting non-structural systems and also to be used as a connector between masonry walls and the main frames, taking advantage of masonry wall resistance capability.

And stable hysteretic behavior has been obtained from tested specimens. All devices give over 75% efficiency when compared to a perfectly elastic plastic device. The 'A' device presents the highest average absolute cumulative angular strain value ($\gamma_T$), indicating that the transition radius does not improve hysteretic behavior of the dissipator. An acceptable reason would be that it reduces web area where dissipation takes place. This conclusion is clear when the ratio r/b is large enough, but and extensive test program have to be done to confirm it.

After web damage has appeared, all devises maintain dissipating energy. This is due to the flanges and stiffeners which are not damaged and they are thick and narrow dimensioned. In a full restrained vertical displacement situation, this sub-structure dissipates energy by bending and by axial forces caused, the later one, by large displacements and second order forces.

If the vertical displacement is restrained, vertical force evolution inflects when web damage appears, increasing its value considerably. Consequences should have to be observed if dissipator is used in real frames.

Main characteristics of the proposed shear link dissipators are well predicted both using simple expressions and numerical models. The numerical simulation of the shear link in SDOF systems was performed using a simple step by step analysis modeling the dissipator as a nonlinear spring. The results indicate a good correlation in main indicative parameters.

## ACKNOWLEDGEMENTS

The support of the European Community under the ECOEST2 program "Training and Mobility of Researchers - Access to Large-Scale models" (contract N.ERBFMGECT950048), and from ISMES is gratefully acknowledged.

## REFERENCES

Bleich, F., (1952), *Buckling Strength of Metal Structures*, McGra-Hill Book Company, New York

Bozzo, L.M.., Foti D. and Lopez-Almansa, F. (1996). "Design Criteria for Earthquake Resistant Buildings with Energy Dissipators", *Proceedings of the Eleventh World Conference on Earthquake Engineering*

Brokken, S., and Bertero, V.V., (1981). "Studies on the Effects of Infills in Seismic Resistant R/C Construction", *UBC/EERC-81/12 Report, Earthquake Engineering Research Center, University of California at Berkeley*.

Cahis, X., Bozzo, L. and Torres Ll. (1998) "Experimental studies of various innovative energy dissipation devices", *Proceedings of the 11th European Conference on Earthquake Engineering*

International Conference of Building Officials (1997), *Uniform Building Code*, Whittier, California

Kasai, K and Popov, E. P. (1986) "Cyclic Web Buckling Control for Shear Link Beams", *Journal of Structural Engineering (ASCE)*, vol. 112, num. 3, pp. 505-523

Roeder, C. W. and Popov, E. P. (1978). "Eccentrically Braced Steel Frames for Earthquakes", *Journal of the Structural Division, ASCE*, Vol.. 104, pp. 391-412.

Rai, D. C. and Wallace, B. J. (1998) "Aluminium Shear-Links for Enhance Seismic Resistance", *Earthquake Engineering and Structural Dynamics*, num. 27, pp. 315-342

Yanev, B., and McNiven, H.D., (1985). "An Experimental Program for Studying the Dynamic Response of a Steel Frame with a Variety of Infill Partitions", *UBC/EERC-85/16 Report, Earthquake Engineering Research Center, University of California at Berkeley*